Biomaterials 31 (2010) 7836–7845

Contents lists available at ScienceDirect

Biomaterials

journal homepage: www.elsevier.com/locate/biomaterials

Enhanced proteolytic degradation of molecularly engineered PEG hydrogels in response to MMP-1 and MMP-2

J. Patterson [a], J.A. Hubbell [a,b,*]

[a] Institute for Bioengineering, Ecole Polytechnique Fédérale de Lausanne (EPFL), Lausanne, Vaud, CH-1015, Switzerland
[b] Institute for Chemical Sciences and Engineering, Ecole Polytechnique Fédérale de Lausanne (EPFL), Lausanne, Vaud, CH-1015, Switzerland

ARTICLE INFO

Article history:
Received 9 June 2010
Accepted 30 June 2010
Available online 27 July 2010

Keywords:
Biodegradation
Biomimetic material
Cell spreading
Hydrogel
Matrix metalloproteinase
Peptide

ABSTRACT

Bioactive hydrogels formed by Michael-type addition reactions of end-functionalized poly(ethylene glycol) macromers with cysteine-containing peptides have been described as extracellular matrix mimetics and tissue engineering scaffolds. Although these materials have shown favorable behavior *in vivo* in tissue repair, we sought to develop materials formulations that would be more rapidly responsive to cell-induced enzymatic remodeling. In this study, protease-sensitive peptides that have increased k_{cat} values were characterized and evaluated for their effects on gel degradability. Biochemical properties for soluble peptides and hydrogels were examined for matrix metalloproteinase (MMP)-1 and MMP-2. The most efficient peptide substrates in some cases overlap and in other cases differ between the two enzymes tested, and a range of k_{cat} values was obtained. For each enzyme, hydrogels formed using the peptides with higher k_{cat} values degraded faster than a reference with lower k_{cat}. Fibroblasts showed increased cell spreading and proliferation when cultured in 3D hydrogels with faster degrading peptides, and more cell invasion from aortic ring segments embedded in the hydrogels was observed. These faster degrading gels should provide matrices that are easier for cells to remodel and lead to increased cellular infiltration and potentially more robust healing *in vivo*.

1. Introduction

When designing an ideal biomaterial matrix or delivery vehicle, the materials should degrade during the course of tissue regeneration so that ultimately no foreign materials would remain. In addition to providing a base structural support to the regenerating tissue or serving as a delivery vehicle for bioactive molecules to stimulate healing, the materials themselves can provide cues to stimulate a cellular response.

Synthetic hydrogels [1–4], including those formed from Michael-type addition reactions of end-functionalized poly (ethylene glycol) (PEG) macromers with cysteine-containing peptides or proteins [5–8], offer several advantages as extracellular matrix (ECM) mimetics and tissue engineering scaffolds including low risk of immune reaction and ease of material handling. Using entirely synthetic or recombinantly produced materials, key features of the ECM, such as the hydrated viscoelastic environment as well as the presentation of matrix-bound and soluble signals, can be recapitulated [1]. PEG hydrogels formed by Michael-addition reactions can be rendered proteolytically sensitive by the incorporation of a matrix metalloproteinase (MMP) substrate sequence and have been explored by our lab to promote cellular migration into the polymer hydrogel [5–8]. To form a cell-responsive hydrogel, vinyl sulfone-terminated multi-arm-PEG first can be functionalized with cysteine-containing cell adhesion ligands, growth factor binding ligands, or growth factors and then is crosslinked into a gel network by protease-sensitive peptide substrates flanked by cysteine-containing domains. When the gels come into contact with cells *in vitro* or *in vivo*, they are locally degraded as the cells respond to cues presented by the gel.

Initial development of these hydrogels utilized the MMP substrate site found within the alpha chain of type I collagen (GPQG↓IAGQ) with a single amino acid substitution (A→W) to enhance activity [9] (throughout, we utilize the symbol ↓ to demarcate the protease cleavage site). Previous research has shown that simple changes to the peptide substrate sequence in the crosslinker could render the hydrogels more or less degradable, with the more rapidly degradable hydrogels leading to more bone formation *in vivo* with increases in both mineralization and cell invasion [8]. Additionally, it has been shown that physiologically

* Corresponding author at: Institute for Bioengineering, Ecole Polytechnique Fédérale de Lausanne (EPFL), Lausanne, Vaud, CH-1015, Switzerland. Fax: +41 21 693 9685.
E-mail address: jeffrey.hubbell@epfl.ch (J.A. Hubbell).

0142-9612/$ – see front matter © 2010 Elsevier Ltd. All rights reserved.
doi:10.1016/j.biomaterials.2010.06.061

normal angiogenesis could be induced by sustained, very low levels of exposure to vascular endothelial growth factor (VEGF), when delivered from these hydrogels [10]. However, for certain tissue repair applications, the remodeling rate of the hydrogels may limit cellular infiltration and may simply be too slow. We hypothesized that increased proteolytic degradation would lead to enhanced cellular invasion responses. To accomplish this, we have sought to find protease substrates that degrade faster or more specifically and to use them as crosslinkers. In this study, the biochemical degradation properties were examined for hydrogels formed with different protease substrates derived from the literature. The ability of faster degrading hydrogels to support enhanced cellular invasion was also tested in several *in vitro* models.

Protease-sensitive PEG based hydrogels have seen wide application [8,11,12]; however, the majority of studies have used the collagen-based GPQG↓IAGQ or GPQG↓IWGQ sequences as the protease substrate. These substrates do not degrade particularly fast and can be cleaved by a number of MMPs. Using combinatorial methods or other design approaches, other groups have found MMP substrate sequences that show increases in enzymatic sensitivity or specificity [13–28]. Examples are shown in Table 1. These include sequences derived from the collagen cleavage sequence,

Table 1
Kinetic parameters for optimized MMP cleavage sequences from the literature.

	k_{cat}/K_M ($M^{-1}s^{-1}$)								
Peptide Sequence	MMP-1	MMP-2	MMP-3	MMP-7	MMP-8	MMP-9	MMP-11	MMP-13	MT1-MMP
GPQG↓IAGQ (30 °C, pH 7.5)	60.6 [9]	180 [9]	16.7 [9]	110 [9]	1570 [9]	93.9 [9]	–	–	–
GPQG↓IWGQ l(30 °C, pH 7.5)	434 [9]	555 [9]	56.0 [9]	–	11,100 [9]	214 [9]	–	–	–
GGGGS-GVPDVGRYSLFP-GGGGS (proMMP; 37 °C)	88.89 [16]	–	177.78 [16]	–	–	–	–	–	–
GPQG↓IAGQ (collagen)	27.4 [17]	10,100 [17]	160 [17]	180 [17]	–	8400 [17]	–	–	3600 [17]
VPMS↓MRGG (optimized for MMP-1)	1600 [17]	24,000 [17]	3900 [17]	7900 [17]	–	51,000 [17]	–	–	6100 [17]
IPVS↓LRSG (optimized for MMP-2)	98 [17]	82,000 [17]	2300 [17]	9700 [17]	–	11,500 [17]	–	–	4300 [17]
RPFS↓MIMG (optimized for MMP-3)	440 [17]	4600 [17]	6900 [17]	12,000 [17]	–	21,000 [17]	–	–	3700 [17]
VPLS↓LTMG (optimized for MMP-7)	300 [17]	13,200 [17]	2400 [17]	120,000 [17]	–	20,000 [17]	–	–	10,300 [17]
VPLS↓LYSG (optimized for MMP-9)	2100 [17]	61,000 [17]	1390 [17]	22,000 [17]	–	49,000 [17]	–	–	5500 [17]
IPES↓LRAG (optimized for MT1-MMP)	870 [17]	24,000 [17]	1500 [17]	12,000 [17]	–	12,600 [17]	–	–	6900 [17]
SGESPAY↓YTA (optimized for MMP-2)	–	440,000 [18]	–	1500 [18]	–	30,000 [18]	–	5300 [18]	–
Ac-GAPFA↓LRLV (Consensus; 37 °C)	–	–	80,000 [19]	61,800 [19]	–	–	–	–	–
Ac-PLE↓LRA-NH_2 (Minimal; 37 °C)	–	–	42,000 [19]	177,000 [19]	–	–	–	–	–
GGYAE↓LRMGG (MMP-11 consensus; 37 °C, pH 7.6)	–	–	–	–	–	–	2030 [20]	–	<200 [20]
GGPLG↓LYAGG (MT1-MMP consensus; 37 °C, pH 7.5)	–	–	–	–	–	–	<20 [20]	–	16,000 [20]
GPLG↓LWAR (optimized for MMP-13; 37 °C, pH 7.5)	30,600 [21]	–	4000 [21]	–	–	103,000 [21]	–	1,410,000 [21]	–
Ac-GPL↓GLRSW (37 °C; 1 h; 100 nM; 125 nM; 400 nM)	–	95.1% [22]	–	–	–	93.1% [22]	–	–	96.8% [22]
Mca-PLGL-Dpa-AR-NH_2 (37 °C; MMP-2 at 25 °C)	14,800 [24]	629,000 [24]	23,000 [24]	169,000 [24]	–	–	–	–	–
Type I Collagen (37 °C)	10.0 (rel.) [25]	–	–	–	–	N.D. [25]	–	–	–
Dnp-P-Cha-Abu↓Smc-HA-DR-NH_2 (37 °C)	36.6 (rel.) [25]	–	–	–	–	1.7 (rel.) [25]	–	–	–
fTHP-3 (triple helical; 30 °C, pH 7.5)	1278 [26]	1082 [26]	503 [26]	–	–	–	–	2273 [26]	–
α1(V)436-447 fTHP (triple helical; 30 °C, pH 7.5)	<48 [27]	14,002 [27]	<48 [27]	–	–	5449 [27]	–	434 [27]	579 [27]
fTHP-4 (triple helical; 30 °C, pH 7.5)	3900 [28]	–	–	–	4500 [28]	–	–	1600 [28]	–
fTHP-9 (triple helical; 30 °C, pH 7.5)	–	–	–	–	175,000 [28]	–	–	25,000 [28]	–
fTHP-11 (triple helical; 30 °C, pH 7.5)	–	–	–	–	19,000 [28]	–	–	13,000 [28]	–

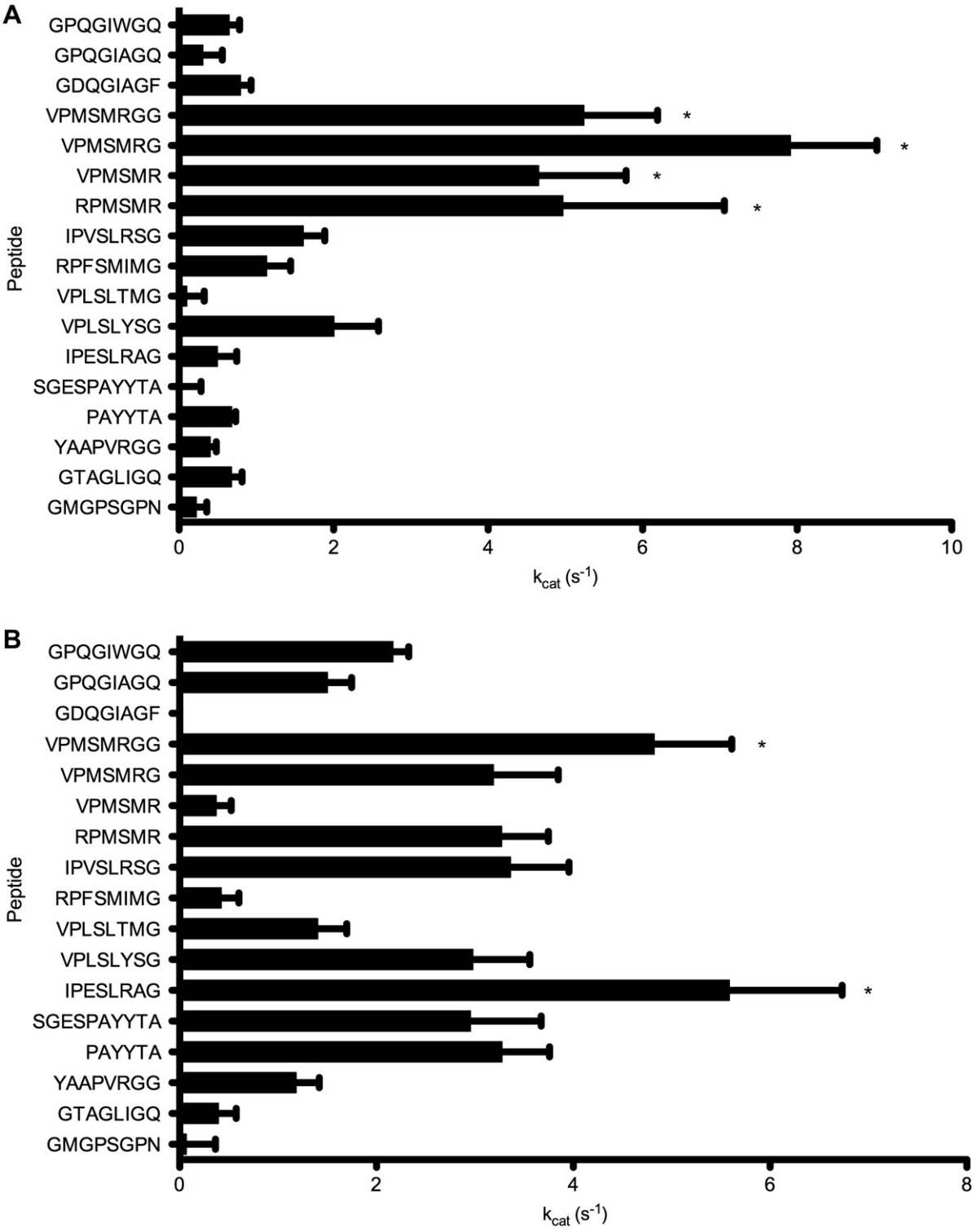

Fig. 1. Measurement of k_{cat} by Michaelis–Menten analysis for soluble peptides degraded by (A) MMP-1 or (B) MMP-2, each at 10 nM. A minimum of triplicate samples was analyzed for each peptide. *indicates statistical significance at $p < 0.05$ (one-way ANOVA followed by Bonferroni's multiple comparison test). Peptides are indicated as the cleavage sequence, but all are flanked by cysteine-containing domains as described in the text.

GPQG↓IAGQ [9], including amino acid substitutions to alter activity [9,13–15]; sequences based on the activation site of pro-MMPs [16]; sequences optimized using mixture-based peptide libraries screened with different MMPs [17]; sequences selected from a phage display library for degradation by MMP-2 [18], by MMP-3 or MMP-7 [19], by MMP-11 [20], by MMP-13 [21], or by MT1-MMP [22]; fluorogenic peptide sequences to facilitate kinetic measurements [23,24]; fluorogenic sequences with natural and non-natural amino acids optimized for MMP-1 or MMP-9 cleavage [25]; and homotrimeric, fluorogenic triple helical peptide (fTHP) models of the MMP-1 cleavage site in type II collagen [26], of the MMP-9 cleavage site in type V collagen [27], or with different thermal stabilities [28].

When selecting a degradation sequence, a substrate that mimics the triple helical nature of collagen would seem like an obvious choice. However, the 5 Å wide collagenase active site is only large enough to accommodate a single polypeptide chain [29], and recent work has shown that MMP-1 locally unwinds the collagen triple helix before hydrolysis [30]. Further, while the triple helical peptides of Lauer-Fields et al. have been shown to be efficient substrates for the MMPs [26–28], their complex fabrication could also limit the cost-effectiveness of their use in the PEG hydrogels. Therefore, substrate sequences discovered by Turk et al. using a combinatorial method of oriented peptide libraries were utilized in this study. These sequences were optimized for degradation by MMP-1, MMP-2, MMP-3, MMP-7, MMP-9, and MT1-MMP and show three-fold to over six hundred-fold increases in the kinetic parameter k_{cat}/K_M (Table 1) compared to the MMP cleavage site GPQG↓IAGQ in collagen [17]. Additional sequences determined from screening phage display libraries for degradation by MMP-2 by Chen et al. were also utilized as these show a k_{cat}/K_M that is six-fold higher than the best sequence determined by Turk et al. and fifty-fold higher than the MMP cleavage site GPQG↓IAGQ in collagen (Table 1).

Finally, three additional peptides were tested. GTAG↓LIGQ was used as a degradable segment in self-assembling peptide amphiphile nanofibers [31]. YAAPV↓RGG was derived from a study to develop human neutrophil elastase responsive PEG hydrogels [32]. Lastly, GMGP↓SGPN was developed as a cathepsin K sensitive peptide [33]. The peptide substrates YAAPV↓RGG and GMGP↓SGPN would be expected not to be particularly sensitive to MMPs.

2. Materials and methods

2.1. PEG-vinyl sulfone (PEG-VS)

Branched four-arm-PEG with a molecular mass of 20 kDa (nominal) was purchased from Nektar (San Carlos, CA) and functionalized at the OH termini, as previously described [6]. Briefly, the PEG was dried by azeotropic distillation in toluene using a Dean Stark trap prior to dissolving in dichloromethane (DCM), which had been dried over molecular sieves. The PEG solution was reacted with NaH and then, after hydrogen evolution, with divinyl sulfone (Fluka) in a molar ratio of OH:NaH:divinyl sulfone of 1:50:75. The reaction was carried out at room temperature under argon with constant stirring for 24–72 h. The reaction solution was neutralized with concentrated acetic acid and filtered until clear. The derivatized polymer was isolated by precipitation in cold diethyl ether and washed. The product was redissolved and reprecipitated with thorough washing two to four more times to remove all excess divinyl sulfone. Finally, the product was dried under vacuum. The derivatization was confirmed with ^{1}H NMR ($CDCl_3$), which showed characteristic vinyl sulfone peaks at 6.1, 6.4, and 6.8 ppm. The degree of end group conversion was calculated based on NMR analysis and was approximately 90%.

2.2. Peptide synthesis

Synthesis chemicals were of analytical grade or better from Novabiochem, Läufelfingen, Switzerland. Peptides were synthesized on solid resin (Novasyn TGR) using the peptide synthesizer PSW 1100 (Chemspeed, Augst, Switzerland) with standard F-moc chemistry (HBTU). After synthesis, the oligopeptides were cleaved from the resin for 2–3 h in a solution of trifluoroacetic acid (Fluka, Buchs, Switzerland), deionized water, 1,2-ethanedithiol (Fluka), and triisopropylsilane (Sigma) in a ratio of 94:2.5:2.5:1. The resin was removed by filtration. Hydrophobic scavengers and cleaved protecting groups were removed by precipitation of the peptide in cold diethyl ether. Purification was performed by C18 chromatography (Prep Nova-Pak HR C_{18} 6 μm, 60 Å, 19 × 300-mm column, Waters, Milford, MA), and peptides were analyzed by matrix-assisted laser desorption ionization/time-of-flight (MALDI-TOF) mass spectrometry. Peptides were lyophilized and stored at −20 °C. The sulfhydryl content of the crosslinker peptide was measured using Ellman's reagent (5,5′-dithio-bis(nitrobenzoic acid); Sigma). Ellman's reagent was dissolved at 4 mg/mL in 0.1 M phosphate buffer, pH 8.0, with 1 mM EDTA. To 20 μL of this solution was added the same buffer containing the peptide. The thiol concentration was determined from a standard curve ranging from 0.1 to 3 mM of thiomalic acid, measuring absorbance at 412 nm.

2.3. Determination of degradation kinetics of soluble peptides by MMP-1 or MMP-2 using Michaelis–Menten analysis

The kinetic parameters of substrate hydrolysis (K_M and k_{cat}) were measured using a fluorometric assay that has been published [8,34]. Briefly, MMP-1 or MMP-2 was incubated with individual substrates at 30 °C in buffer solution (50 mM tricine, 50 mM NaCl, 10 mM $CaCl_2$ and 0.05% Brij-35, pH 7.5) followed by reaction with fluorescamine and detection of the fluorescence ($\lambda_{excitation} = 387$ nm, $\lambda_{emission} = 480$ nm) on a Tecan Safire spectrofluorometer. Initial reaction velocities were obtained from plots of fluorescence vs. time, and the kinetic parameters (K_M and k_{cat}) were determined by fitting rate vs. substrate concentration data to the Michaelis–Menten equation using the software package GraphPad Prism.

2.4. Formation of PEG based hydrogels

Preparation of hydrogels was accomplished through Michael-type addition reaction of thiol-containing peptides onto PEG-VS, as described by Lutolf et al. [5–8]. A typical cell-adhesive, MMP-sensitive gel of 50 μL volume containing 10% (w/v) PEG was formed by dissolving 5 mg PEG in 20 μL HEPES buffer (0.3 M, pH 8.0) or triethanolamine buffer (0.3 M, pH 8.0) and reacting this solution with 5 μL of 5 mM RGD (Ac-G**C**GYGRGDSPG-NH_2; in the same buffer) in a first step at 37 °C for 30 min. The monocysteine species were always added at far less than equivalence, and thus the majority of the reactions with the functionalized PEG yielded singly reacted PEG. This solution was then mixed with 25 μL of a solution (in the same buffer) containing a peptide with a protease substrate sequence (usually of the form Ac-G**C**RD-XXXX↓XXXX-DR**C**G-NH_2). Gelation occurred within a few minutes; however, the crosslinking reaction was continued for 30 min at 37 °C in a humidified incubator. The amounts of reactive thiols and vinyl sulfone groups in this crosslinking mix were stoichiometrically balanced. The protease-sensitive sequences were taken from the literature (see Tables 1 and 3). Generally, RD sequences flanking the reactive cysteine residues were added to improve peptide solubility in water and provide an optimal pK_a for reactivity [6,35].

2.4.1. Preparation of disk-shaped samples

After mixing, the precursor solution was pipetted onto a sterile hydrophobic glass microscope slide (coated with SigmaCote; Sigma) with approximately 1 mm thick spacers at both ends. A second hydrophobic glass microscope slide was positioned and clamped with binder clips over the lower slide so that the drop of precursor solution spread to form a disk between the two hydrophobic surfaces. The crosslinking reaction was allowed to proceed for 30 min at 37 °C in a humidified atmosphere. The hydrogels were then stored in buffers of choice for further investigation.

2.5. Biochemical degradation of hydrogels

Hydrogels obtained from 5 or 10 μL of precursor solution were incubated at 37 °C in suitable buffer (50 mM tricine, 50 mM NaCl, 10 mM $CaCl_2$ and 0.05% Brij-35, pH 7.5) with MMP-1 or MMP-2. Proteolytic degradation of the hydrogels was monitored by measuring the time to complete hydrogel degradation.

Table 2
Comparison of measured k_{cat} to literature values.

Enzyme	Peptide k_{cat} (s^{-1}) [9]	Peptide k_{cat} (s^{-1}) [8]	Peptide k_{cat} (s^{-1}) [measured]
MMP-1	GPQG↓IAGQ 0.20	Ac-G**C**RD-GPQG↓IAGQ-DR**C**G-NH_2 0.17 ± 0.03	Ac-G**C**RD-GPQG↓IAGQ-DR**C**G-NH_2 0.31 ± 0.25
MMP-1	GPQG↓IWGQ 0.36	Ac-G**C**RD-GPQG↓IWGQ-DR**C**G-NH_2 0.51 ± 0.10	Ac-G**C**RE-GPQG↓IWGQ-ER**C**G-NH_2 0.65 ± 0.13
MMP-2	GPQG↓IAGQ 2.7		Ac-G**C**RD-GPQG↓IAGQ-DR**C**G-NH_2 1.50 ± 0.25
MMP-2	GPQG↓IWGQ 0.61		Ac-G**C**RE-GPQG↓IWGQ-ER**C**G-NH_2 2.17 ± 0.16

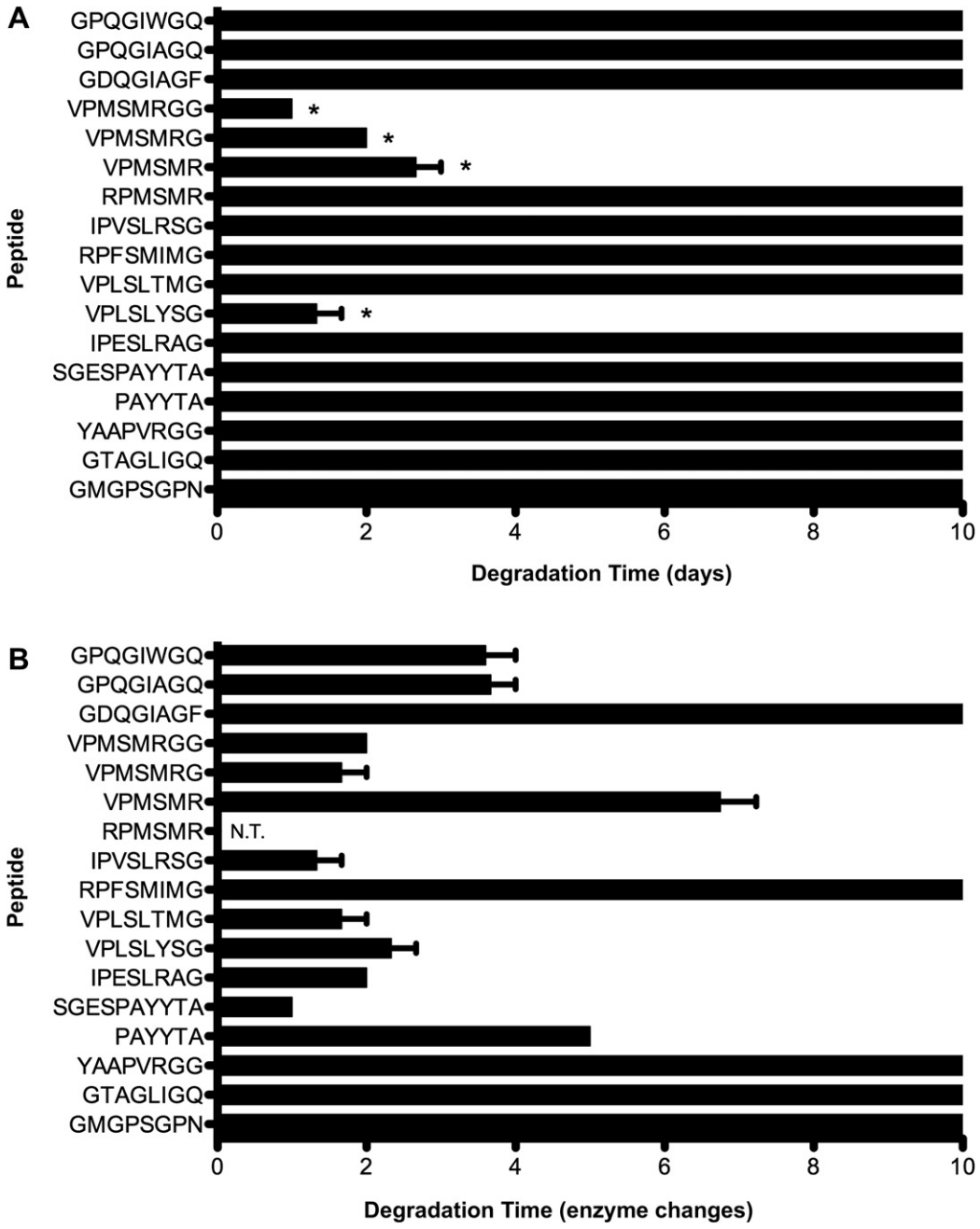

Fig. 2. Measurement of hydrogel degradation by (A) MMP-1 at 10 nM or (B) MMP-2 at 20 nM. For each graph, the time axis was truncated, although gels that reached this maximum all persisted longer. A minimum of triplicate samples was analyzed for each peptide. *indicates statistical significance at $p < 0.05$ (one-way ANOVA followed by Bonferroni's multiple comparison test). N.T. indicates sample was not tested. Peptides are indicated as the cleavage sequence, but all are flanked by cysteine-containing domains as described in the text.

2.6. Cell proliferation and spreading

To assess the proliferation and spreading of fibroblasts inside MMP-sensitive PEG hydrogels, primary mouse myofibroblasts transfected with the fluorescent protein tomato were suspended within the precursor solution at 2.5×10^5 cells/mL. Cells were mixed with the crosslinker solution immediately before hydrogel formation, replacing about 20% of the precursor solution volume. The gels were placed in low-binding 96-well plates with 150 μL of fibroblast growth medium and were incubated at 37 °C for up to 3 wk. At each time point, cell spreading in 3D was examined using confocal microscopy (Zeiss LSM 700), and cell proliferation was measured using an MTS assay kit (Promega). The gels containing cells were incubated with 150 μL medium and 30 μL MTS solution for 2 h. The absorbance at 490 nm was then measured for a 100 μL aliquot of the media.

2.7. Chick aortic ring model

A chick aortic ring outgrowth assay was performed to examine cell invasion into the hydrogels. Day 8–10 chicken embryos were sacrificed, and the major blood vessels coming from the heart were removed and rinsed in endothelial basal medium (Lonza). The isolated vessels were cleaned of adipose tissue and cut into small segments with a scalpel. A base hydrogel layer that was approximately 300 μm thick was prepared from 4 μL precursor solution without RGD to ensure that cells would not grow out of the gel and onto the dish. After the base layer had gelled, a second 10 μL gel (approximately 1 mm thick) was formed on top, and one aortic segment was placed in the gel solution immediately after mixing. After polymerization of the gels at 37 °C for 30 min, they were transferred to 48-well plates with 300 μL of endothelial cell growth medium. After 2 h of incubation to allow for gel

Table 3
Summary of kinetic parameters measured for soluble peptides and hydrogel degradation times for MMP-1 and MMP-2. N.D. indicates k_{cat} was below detectable limits. N.T. indicates sample was not tested. Values in bold show both higher k_{cat} and faster degradation time than the reference peptide. Peptides in italics were further examined in cell proliferation assays. *indicates statistical significance at $p < 0.05$ (one-way ANOVA followed by Bonferroni's multiple comparison test) compared to the reference peptide. N.D. indicates value was too low to measure.

Peptide sequence	k_{cat} (s^{-1}) MMP-1	Deg. time MMP-1	k_{cat} (s^{-1}) MMP-2	Deg. time MMP-2
*Ac-G**C**RE-GPQG↓IWGQ-ER**C**G-NH$_2$*	*0.65 ± 0.13*	*10+*	*2.17±0.16*	*3.6*
Ac-G**C**RD-GPQG↓IAGQ-DR**C**G-NH$_2$	0.31 ± 0.25	10+	1.50 ± 0.25	3.7
Ac-G**C**RD-GDQG↓IAGF-DR**C**G-NH$_2$	0.79 ± 0.14	10+	N.D.	10+
*Ac-G**C**RD-VPMS↓MRGG-DR**C**G-NH$_2$*	***5.25 ± 0.95****	***1.0****	***4.82 ± 0.79****	***2.0***
Ac-G**C**D-VPMS↓MRG-D**C**G-NH$_2$	**7.91 ± 1.12***	**2.0***	**3.19 ± 0.66**	**1.7**
Ac-G**C**D-VPMS↓MR-D**C**G-NH$_2$	**4.66 ± 1.13***	**2.7***	0.37 ± 0.15	6.8
*Ac-G**C**-RPMS↓MR-**C**G-NH$_2$*	*4.97 ± 2.09**	*10+*	*3.27 ± 0.47*	*N.T.*
Ac-G**C**RD-IPVS↓LRSG-DR**C**G-NH$_2$	1.61 ± 0.28	10+	**3.36 ± 0.59**	**1.3**
*Ac-G**C**RD-RPFS↓MIMG-DR**C**G-NH$_2$*	*1.14 ± 0.31*	*10+*	*0.42 ± 0.18*	*10+*
Ac-G**C**RD-VPLS↓LTMG-DR**C**G-NH$_2$	0.10 ± 0.23	10+	1.40 ± 0.30	1.7
Ac-G**C**RD-VPLS↓LYSG-DR**C**G-NH$_2$	**2.01 ± 0.58**	**1.3***	**2.98 ± 0.58**	**2.3**
*Ac-G**C**RD-IPES↓LRAG-DR**C**G-NH$_2$*	*0.50 ± 0.25*	*10+*	***5.59 ± 1.14****	***2.0***
Ac-G**C**RD-SGESPAY↓YTA-DR**C**G-NH$_2$	0.03 ± 0.25	10+	**2.96 ± 0.72**	**1.0**
Ac-G**C**D-PAY↓YTA-D**C**G-NH$_2$	0.68 ± 0.05	10+	3.27 ± 0.48	5.0
Ac-G**C**RD-YAAPV↓RGG-DR**C**G-NH$_2$	0.41 ± 0.08	10+	1.18 ± 0.24	10+
*Ac-G**C**RD-GTAG↓LIGQ-DR**C**G-NH$_2$*	*0.68 ± 0.13*	*10+*	*0.39 ± 0.18*	*10+*
Ac-G**C**RD-GMGP↓SGPN-DR**C**G-NH$_2$	0.22 ± 0.13	10+	0.07 ± 0.30	10+

swelling, the medium was removed and replaced with 300 μL of fresh medium. Outgrowth from the rings was imaged using phase contrast microscopy at several time points, and the culture medium was changed regularly.

2.8. Statistical analysis

Experiments were conducted with a minimum of triplicate samples. Data were analyzed using the GraphPad Prism software package. One or two factor ANOVAs with appropriate post-tests were performed as indicated in the results. Differences were considered statistically significant when the *p*-value was less than 0.05.

3. Results

3.1. Kinetic parameters for degradation of soluble peptides by MMP-1 or MMP-2

The kinetic parameter, k_{cat}, was measured for each of the peptides in soluble form. All peptides were compared to the Ac-G**C**RE-GPQG↓IWGQ-ER**C**G-NH$_2$ peptide, the degradable peptide used in our previous studies [8], as a reference. Four peptides had significantly higher k_{cat} values relative to the reference sequence when degraded by MMP-1 (Fig. 1A), about four- to eight-fold higher. These peptide sequences are variants of an optimized peptide (VPMS↓MRGG) from an oriented peptide library screened for degradation by MMP-1 [17]. Three additional peptides had smaller but statistically insignificant increases in k_{cat}. The k_{cat} values measured for two of the collagen-derived peptides (Ac-G**C**RD-GPQG↓IAGQ-DR**C**G-NH$_2$ and Ac-G**C**RE-GPQG↓IWGQ-ER**C**G-NH$_2$) compare well with k_{cat} values reported in the literature, both for the eight amino acid cleavage sequences [9] and for the cleavage sequences flanked by cysteine-containing domains [8], as summarized in Table 2.

Soluble peptide degradation by MMP-2 identified two peptides with significantly increased k_{cat} values (Fig. 1B). These peptide sequences (VPMS↓MRGG and IPES↓LRAG) came from a peptide library screened for degradation by different MMPs [17], and these two peptides were actually discovered when optimizing for degradation by MMP-1 and MT1-MMP, respectively. Interestingly, while not statistically significant, almost all of the peptides derived from the library screenings had some increase in k_{cat} compared to the reference sequence (Ac-G**C**RE-GPQG↓IWGQ-ER**C**G-NH$_2$). Again, the k_{cat} values for two of the collagen-derived peptides compare well with the literature (Table 2).

3.2. Enzymatic degradation of hydrogels

Hydrogels formed from the different crosslinker peptides were degraded by exposure to MMP-1 or MMP-2. It was expected that peptides with higher k_{cat} values would result in hydrogels with faster degradation times than ones formed with the reference peptide (Ac-G**C**RE-GPQG↓IWGQ-ER**C**G-NH$_2$). The results of the degradation of hydrogels by MMP-1 can be seen in Fig. 2A. The axis showing degradation time is truncated at 10 d, but the gels that reached this point all persisted longer. Four gels had significantly faster degradation times than the control, and these peptide sequences matched with those found to have higher k_{cat} values. Table 3 summarizes the k_{cat} and hydrogel degradation

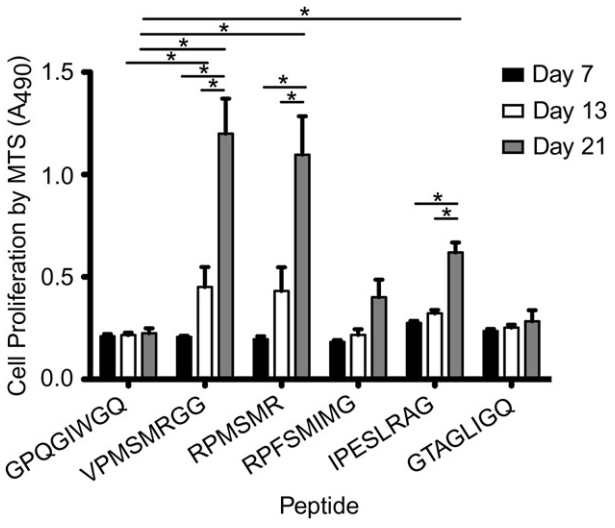

Fig. 3. Measurement of mouse myofibroblast proliferation in 3D PEG hydrogels containing different protease substrates as crosslinkers. Cell proliferation was measured by an MTS assay. Cells were seeded at 2.5×10^5 cells/mL in a precursor solution that contained 6.5% PEG-VS and 500 μM RGD peptide with stoichiometric amounts of crosslinker peptide. A minimum of triplicate samples was analyzed for each peptide. *indicates statistical significance at $p < 0.05$ (two-way ANOVA followed by Bonferroni's post-test). Peptides are indicated as the cleavage sequence, but all are flanked by cysteine-containing domains as described in the text.

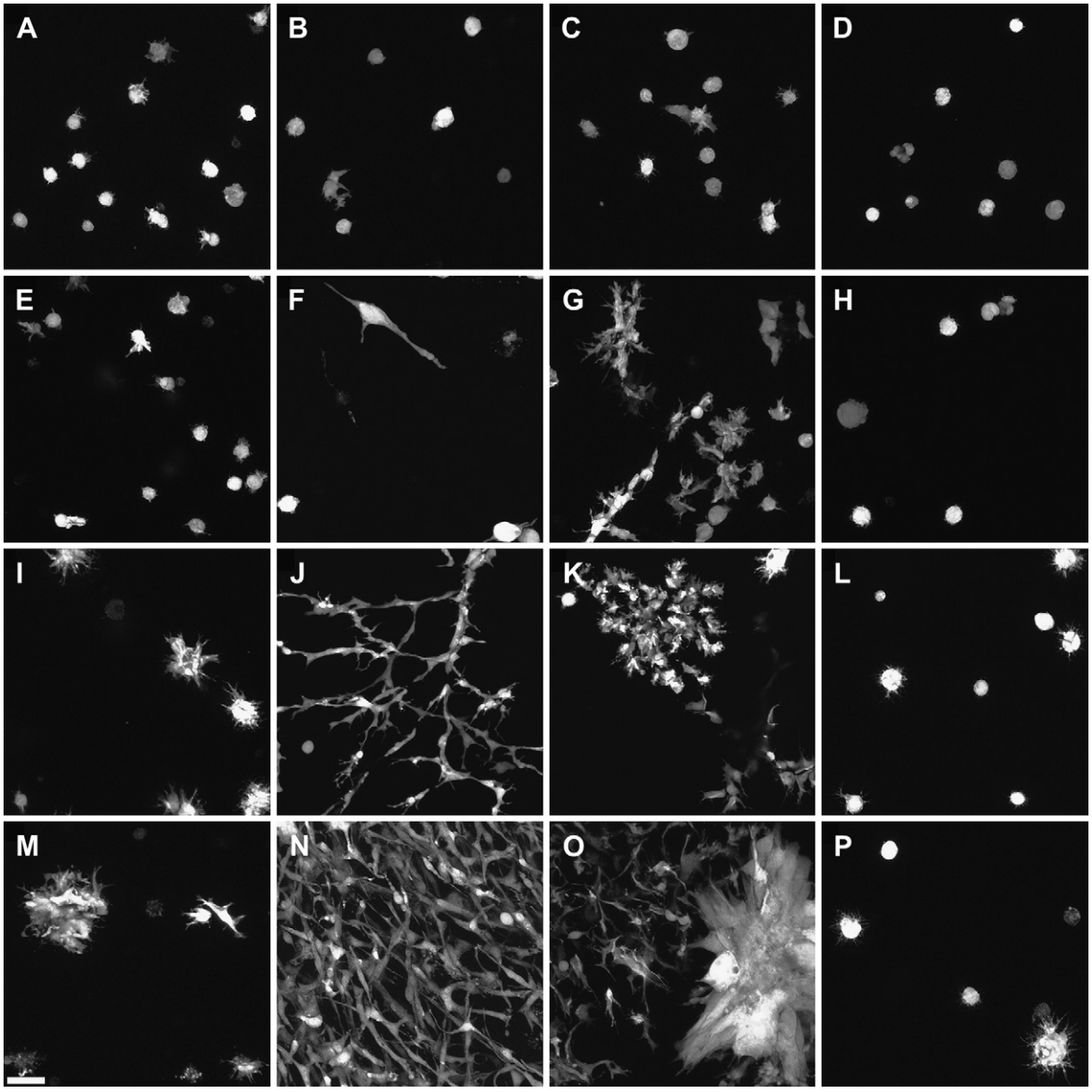

Fig. 4. Visualization of mouse myofibroblast spreading and proliferation in 3D PEG hydrogels using confocal microscopy. Cells were transfected with the fluorescent protein tomato for visualization. Cells were seeded at 2.5×10^5 cells/mL in a precursor solution that contained 6.5% PEG-VS and 500 μM RGD peptide with stoichiometric amounts of crosslinker peptide. Images were taken using a Zeiss LSM 700 confocal microscope with a 10× objective. The scale bar is 50 μm. (A–D) Day 3. (E–H) Day 7. (I–L) Day 13. (M–P) Day 21. (A,E,I,M) Crosslinker Ac-G**C**RE-GPQG↓IWGQ-ER**C**G-NH_2. (B,F,J,N) Crosslinker Ac-G**C**RD-VPMS↓MRGG-DR**C**G-NH_2. (C,G,K,O) Crosslinker Ac-G**C**RD-IPES↓LRAG-DR**C**G-NH_2. (D,H,L,P) Crosslinker Ac-G**C**RD-GTAG↓LIGQ-DR**C**G-NH_2.

findings for MMP-1, and those peptides with increased k_{cat} values that also resulted in faster degradation are in bold.

For hydrogel degradation with 20 nM MMP-2, four peptides resulted in hydrogels with faster degradation times (Fig. 2B). Three of these four peptides were also found to have higher k_{cat} values than the control. Because MMP-2 inactivates fairly rapidly, the degradation buffer containing MMP-2 was changed daily. The degradation time is therefore reported as the number of enzyme changes until full degradation, and the study was terminated after 10 enzyme changes. Table 3 again summarizes the k_{cat} and hydrogel degradation findings for MMP-2.

Summarizing the biochemical data (Table 3), candidate peptides for faster degradation were identified. The peptide sequences come from different sources in the literature, predominantly peptide libraries screened for degradation by different MMPs. For each enzyme, a range of k_{cat} values was obtained. The increases in k_{cat} correspond well with faster degradation times of hydrogels formed with the different peptides (highlighted in bold in Table 3). Additionally, there are certain peptide sequences that appear specific to one enzyme, while others are susceptible to both of the enzymes tested.

3.3. Fibroblast spreading and proliferation in vitro

To determine if the increases in k_{cat} and gel degradation rate translate to a better functional response at the cellular level, the ability of cells to remodel the hydrogel matrix in 3D was examined. Peptides expected to degrade both faster or slower than the Ac-G**C**RE-GPQG↓IWGQ-ER**C**G-NH_2 peptide were chosen (highlighted in italics in Table 3), and mouse myofibroblasts were embedded in hydrogels

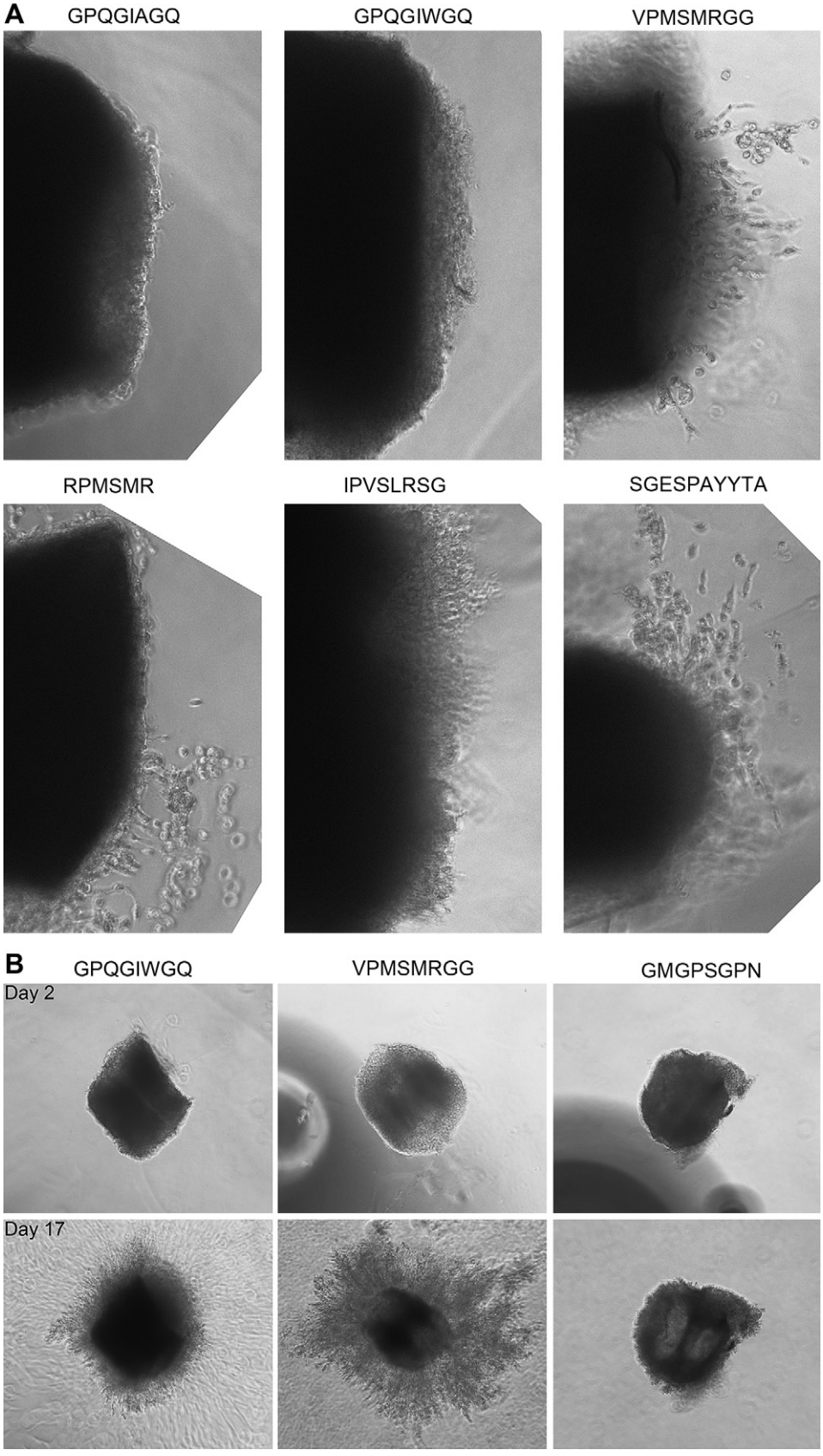

Fig. 5. Visualization of cell invasion into 3D PEG hydrogels using a chick aortic ring outgrowth assay. Segments were cut from aortae dissected from embryonic day 8–10 chicks and embedded in a precursor solution that contained 6.5% PEG-VS and 500 μM RGD peptide with stoichiometric amounts of crosslinker peptide. (A) Cell invasion into the gel was examined by phase contrast microscopy after 48 h. (B) Cell invasion after 48 h and 17 d. Peptides are indicated as the cleavage sequence, but all are flanked by cysteine-containing domains as described in the text.

formed with these peptides. Little cell proliferation occurred with time in the reference and slow degrading samples while the faster degrading peptides led to significant cell proliferation after 2 and 3 wk, compared both to earlier time points and to the reference (Fig. 3). Gels with high and intermediate levels of proliferation were observed, and these corresponded with peptides that had k_{cat} values for MMP-1 that were highly and intermediately increased, respectively.

The morphology of the cells within the hydrogels was examined using confocal microscopy (Fig. 4). Representative images are shown from hydrogels made with the reference peptide, a peptide that resulted in high cell proliferation, one that resulted in intermediate cell proliferation, and one that resulted in little cell proliferation. Several interesting trends were observed in the images. At early time points, there was a rather uniform distribution of cells. For the faster degrading peptides, increased cell spreading (used throughout in the three-dimensional sense) was seen even at early time points. At later time points, extensive cell spreading as well as the effects of cell proliferation were observed. In the slow degrading samples, there was reduced cell spreading and minimal proliferation, even at the later time points.

3.4. Ex vivo chick aortic ring assay

While it is important that cells can spread and proliferate in the degradable hydrogels, for certain applications cells will ultimately need to migrate into the gels from the surrounding tissue. Cell invasion into the hydrogels was tested using a chick aortic ring outgrowth assay. Segments of the aorta of a chicken embryo were embedded in the hydrogels, and cell invasion was examined using microscopy. The images shown (Fig. 5A) are representative micrographs at early time points from hydrogels made with the reference peptide (Ac-G**C**RE-GPQG↓IWGQ-ER**C**G-NH_2), hydrogels made with a slower degrading peptide (Ac-G**C**RD-GPQG↓IAGQ-DR**C**G-NH_2), and hydrogels made with four different faster degrading peptides (Ac-G**C**RD-VPMS↓MRGG-DR**C**G-NH_2, Ac-G**C**-RPMS↓MR-**C**G-NH_2, Ac-G**C**RD-IPVS↓LRSG-DR**C**G-NH_2, and Ac-G**C**RD-SGESPAY↓YTA-DR**C**G-NH_2). No cell invasion was observed with the reference or slow degrading peptides after 48 h, while the beginnings of cell invasion into the hydrogels made with the faster degrading peptides could be seen. In a second study, comparing the reference peptide (Ac-G**C**RE-GPQG↓IWGQ-ER**C**G-NH_2) with a faster degrading peptide (Ac-G**C**RD-VPMS↓MRGG-DR**C**G-NH_2) and a slower degrading peptide (Ac-G**C**RD-GMGP↓SGPN-DR**C**G-NH_2), early differences in cell invasion resulted in differences in radial migration observed after $\geq$ 2 wk of culture (Fig. 5B). The faster degrading hydrogel had the most cell migration, the reference hydrogel had some cell migration, and the slower degrading hydrogel had almost no cell migration.

4. Discussion

In this study, several protease-sensitive peptides that have increased k_{cat} values compared to the MMP cleavage sequence in type I collagen (used as a reference benchmark herein) were utilized to render molecularly engineered PEG hydrogels more degradable. These peptides were chosen from the literature based on their kinetic parameters (Table 1) and were expected to degrade faster than the collagen-based peptides. The sequences tested are summarized in Table 3. In most cases, an eight amino acid long protease substrate sequence was flanked by two cysteine-containing domains (both G**C**RD or both G**C**RE) to result in a sixteen amino acid long crosslinker peptide (Ac-G**C**RD(E)-XXXXXXXX-D(E)R**C**G-NH_2). The amino acids immediately surrounding the cysteine have been shown to influence the kinetics of the Michael-type reaction [6,35], and the sequence G**C**RD was chosen to balance a fast reaction with sufficient time to manipulate the material before the onset of gelation. Because shorter peptides would be easier and more cost efficient to produce, several truncated protease substrates flanked by shorter cysteine-containing domains (G**C**D or G**C**) were also examined.

Here, our biochemical analysis has focused on the kinetic parameter, k_{cat}, and not on K_M or the ratio k_{cat}/K_M because previous work has shown that degradation within the hydrogel is independent of K_M since the substrate concentration there is high and would saturate the enzyme [8]. For the peptides taken from library screenings published in the literature, the trends in k_{cat} for MMP-1 followed what would have been expected given the trends in k_{cat}/K_M with the best performing peptides (variants of VPMS↓MRGG) having up to 8-fold increases in k_{cat}. Peptides from the library screenings also showed increased susceptibility to MMP-2, with the best performing peptides having about a 2-fold increase in k_{cat}. This increase was not as large as could have been expected given the high values reported for k_{cat}/K_M for some of the library-optimized peptides. It is important to note that the cysteine-containing domains were present in the soluble peptides tested here, and these may have an effect on the interactions of the enzymes with some of the substrates.

Screening this collection of peptide substrates has resulted in the ability to tune the degradability of the PEG hydrogels for a specific application. For each enzyme, a range of k_{cat} values was obtained. Efficient substrates in some cases overlap and in other cases differ between the two enzymes tested. For example, the peptides Ac-G**C**RD-VPMS↓MRGG-DR**C**G-NH_2 and Ac-G**C**-RPMS↓MR-**C**G-NH_2 have increased k_{cat} values for both enzymes, while Ac-G**C**RD-IPES↓LRAG-DR**C**G-NH_2 and Ac-G**C**RD-SGESPAY↓YTA-DR**C**G-NH_2 are fairly specific for MMP-2. The peptides result in hydrogels that degrade faster when exposed to the appropriate enzyme(s) and lead to increased cell spreading and cell invasion *in vitro*. The graded increases in k_{cat} and the differential responses for MMP-1 and MMP-2 can be used to engineer hydrogels with degradation properties tuned to the enzymes that are most highly expressed by the relevant cell types of interest. For example, Seliktar et al. showed that endothelial cells predominantly express MMP-2 and MMP-9 while fibroblasts also express MMP-1 and MMP-3 [36]. Further, Brooks et al. demonstrated that active MMP-2 binds the integrin $\alpha_V\beta_3$ on endothelial cells, facilitating matrix degradation in the context of cellular migration [37]. Therefore, peptide sequences optimized for cleavage by MMP-2 could be incorporated into the PEG hydrogels as the degradable linker to target endothelial cell invasion for angiogenesis applications.

5. Conclusions

In this study, peptides from a collection of 17 literature-derived protease substrates were screened for enhanced degradability both in soluble form and in the context of biodegradable crosslinkers within molecularly engineered PEG hydrogels. The most efficient substrates in some cases overlap and in other cases differ between MMP-1 and MMP-2, and a range of k_{cat} values was obtained for each enzyme. The peptides result in hydrogels that degrade faster when exposed to the appropriate enzyme(s) and lead to increased cell spreading and cell invasion *in vitro*. The graded increases in k_{cat} and the differential responses for various enzymes can be used to engineer hydrogels with degradation properties tuned to the enzymes produced by particular cell types. These faster degrading hydrogels should provide a matrix that is easier for cells to remodel and should lead to increased cellular infiltration and ultimately more robust healing *in vivo*.

Acknowledgements

This work was supported in part by a Whitaker International Fellowship to J. Patterson.

References

[1] Patterson J, Martino MM, Hubbell JA. Biomimetic materials in tissue engineering. Mater Today 2010;13:14–22.
[2] Tibbitt MW, Anseth KS. Hydrogels as extracellular matrix mimics for 3D cell culture. Biotechnol Bioeng 2009;103:655–63.
[3] Lin CC, Anseth KS. PEG hydrogels for the controlled release of biomolecules in regenerative medicine. Pharm Res 2009;26:631–43.
[4] Jia X, Kiick KL. Hybrid multicomponent hydrogels for tissue engineering. Macromol Biosci 2009;9:140–56.
[5] Lutolf MP, Raeber GP, Zisch AH, Tirelli N, Hubbell JA. Cell-responsive synthetic hydrogels. Adv Mater 2003;15:888–92.
[6] Lutolf MP, Hubbell JA. Synthesis and physicochemical characterization of end-linked poly(ethylene glycol)-co-peptide hydrogels formed by Michael-type addition. Biomacromolecules 2003;4(3):713–22.
[7] Lutolf MP, Weber FE, Schmoekel HG, Schense JC, Kohler T, Müller R, et al. Repair of bone defects using synthetic mimetics of collagenous extracellular matrices. Nat Biotechnol 2003;21(5):513–8.
[8] Lutolf MP, Lauer-Fields JL, Schmoekel HG, Metters AT, Weber FE, Fields GB, et al. Synthetic matrix metalloproteinase-sensitive hydrogels for the conduction of tissue regeneration: engineering cell-invasion characteristics. Proc Natl Acad Sci U S A 2003;100(9):5413–8.
[9] Nagase H, Fields GB. Human matrix metalloproteinase specificity studies using collagen sequence-based synthetic peptides. Biopolymers 1996;40(4):399–416.
[10] Zisch AH, Lutolf MP, Ehrbar M, Raeber GP, Rizzi SC, Davies N, et al. Cell-demanded release of VEGF from synthetic, biointeractive cell ingrowth matrices for vascularized tissue growth. FASEB J 2003;17(15):2260–2.
[11] Phelps EA, Landazuri N, Thul PM, Taylor WR, Garcia AJ. Bioartificial matrices for therapeutic vascularization. Proc Natl Acad Sci U S A 2010;107:3323–8.
[12] Miller JS, Shen CJ, Legant WR, Baranski JD, Blakely BL, Chen CS. Bioactive hydrogels made from step-growth derived PEG-peptide macromers. Biomaterials 2010;31:3736–43.
[13] Netzel-Arnett S, Fields GB, Birkedal-Hansen H, Wart HEV, Fields G. Sequence specificities of human fibroblast and neutrophil collagenases. J Biol Chem 1991;266(11):6747–55.
[14] Netzel-Arnett S, Sang QX, Moore WG, Navre M, Birkedal-Hansen H, Wart HEV. Comparative sequence specificities of human 72- and 92-kDa gelatinases (type IV collagenases) and PUMP (matrilysin). Biochemistry 1993;32(25):6427–32.
[15] Liu S, Netzel-Arnett S, Birkedal-Hansen H, Leppla SH. Tumor cell-selective cytotoxicity of matrix metalloproteinase-activated anthrax toxin. Cancer Res 2000;60(21):6061–7.
[16] Vessillier S, Adams G, Chernajovsky Y. Latent cytokines: development of novel cleavage sites and kinetic analysis of their differential sensitivity to MMP-1 and MMP-3. Protein Eng Des Sel 2004;17(12):829–35.
[17] Turk BE, Huang LL, Piro ET, Cantley LC. Determination of protease cleavage site motifs using mixture-based oriented peptide libraries. Nat Biotechnol 2001;19(7):661–7.
[18] Chen EI, Kridel SJ, Howard EW, Li W, Godzik A, Smith JW. A unique substrate recognition profile for matrix metalloproteinase-2. J Biol Chem 2002;277(6):4485–91.
[19] Smith MM, Shi L, Navre M. Rapid identification of highly active and selective substrates for stromelysin and matrilysin using bacteriophage peptide display libraries. J Biol Chem 1995;270(12):6440–9.
[20] Pan W, Arnone M, Kendall M, Grafstrom RH, Seitz SP, Wasserman ZR, et al. Identification of peptide substrates for human MMP-11 (stromelysin-3) using phage display. J Biol Chem 2003;278(30):27820–7.
[21] Deng SJ, Bickett DM, Mitchell JL, Lambert MH, Blackburn RK, Carter HL, et al. Substrate specificity of human collagenase 3 assessed using a phage-displayed peptide library. J Biol Chem 2000;275(40):31422–7.
[22] Ohkubo S, Miyadera K, Sugimoto Y, Matsuo K, Wierzba K, Yamada Y. Substrate phage as a tool to identify novel substrate sequences of proteases. Comb Chem High Throughput Screen 2001;4(7):573–83.
[23] Netzel-Arnett S, Mallya SK, Nagase H, Birkedal-Hansen H, Wart HEV. Continuously recording fluorescent assays optimized for five human matrix metalloproteinases. Anal Biochem 1991;195(1):86–92.
[24] Knight CG, Willenbrock F, Murphy G. A novel coumarin-labelled peptide for sensitive continuous assays of the matrix metalloproteinases. FEBS Lett 1992;296(3):263–6.
[25] McGeehan GM, Bickett DM, Green M, Kassel D, Wiseman JS, Berman J. Characterization of the peptide substrate specificities of interstitial collagenase and 92-kDa gelatinase. Implications for substrate optimization. J Biol Chem 1994;269(52):32814–20.
[26] Lauer-Fields JL, Broder T, Sritharan T, Chung L, Nagase H, Fields GB. Kinetic analysis of matrix metalloproteinase activity using fluorogenic triple-helical substrates. Biochemistry 2001;40(19):5795–803.
[27] Lauer-Fields JL, Sritharan T, Stack MS, Nagase H, Fields GB. Selective hydrolysis of triple-helical substrates by matrix metalloproteinase-2 and -9. J Biol Chem 2003;278(20):18140–5.
[28] Minond D, Lauer-Fields JL, Cudic M, Overall CM, Pei D, Brew K, et al. The roles of substrate thermal stability and P2 and P1′ subsite identity on matrix metalloproteinase triple-helical peptidase activity and collagen specificity. J Biol Chem 2006;281(50):38302–13.
[29] Bode W. A helping hand for collagenases: the haemopexin-like domain. Structure 1995;3(6):527–30.
[30] Chung L, Dinakarpandian D, Yoshida N, Lauer-Fields JL, Fields GB, Visse R, et al. Collagenase unwinds triple-helical collagen prior to peptide bond hydrolysis. EMBO J 2004;23(15):3020–30.
[31] Jun HW, Yuwono V, Paramonov SE, Hartgerink JD. Enzyme-mediated degradation of peptide-amphiphile nanofiber networks. Adv Mater 2005;17:2612–7.
[32] Aimetti AA, Tibbitt MW, Anseth KS. Human neutrophil elastase responsive delivery from poly(ethylene glycol) hydrogels. Biomacromolecules 2009;10:1484–9.
[33] Olabisi RMR, Hsu CW, Davis AR, Olmsted-Davis EA, West JL. Cathepsin K sensitive poly(ethylene) glycol hydrogels for degradation in response to bone formation. In: Society for Biomaterials Annual Meeting; 2009.
[34] Lauer-Fields JL, Tuzinski KA, Shimokawa K, Nagase H, Fields GB. Hydrolysis of triple-helical collagen peptide models by matrix metalloproteinases. J Biol Chem 2000;275(18):13282–90.
[35] Lutolf MP, Tirelli N, Cerritelli S, Cavalli L, Hubbell JA. Systematic modulation of michael-type reactivity of thiols through the use of charged amino acids. Bioconjug Chem 2001;12(6):1051–6.
[36] Seliktar D, Zisch AH, Lutolf MP, Wrana JL, Hubbell JA. MMP-2 sensitive, VEGF-bearing bioactive hydrogels for promotion of vascular healing. J Biomed Mater Res A 2004;68(4):704–16.
[37] Brooks PC, Strömblad S, Sanders LC, von Schalscha TL, Aimes RT, Stetler-Stevenson WG, et al. Localization of matrix metalloproteinase MMP-2 to the surface of invasive cells by interaction with integrin alpha v beta 3. Cell 1996;85(5):683–93.